Immunity, Vol. 15, 1039–1049, December, 2001, Copyright ©2001 by Cell Press

Conformational Plasticity Revealed by the Cocrystal Structure of NKG2D and Its Class I MHC-like Ligand ULBP3

Sergei Radaev,[1] Bertha Rostro,[1] Andrew G. Brooks,[2] Marco Colonna,[3] and Peter D. Sun[1,4]

[1] Structural Biology Section
Laboratory of Immunogenetics
National Institute of Allergy and Infectious Diseases
National Institutes of Health
12441 Parklawn Drive
Rockville, Maryland 20852

[2] Department of Microbiology and Immunology
University of Melbourne
Royal Parade
Parkville 3052, Victoria
Australia

[3] Department of Pathology and Immunology
Washington University School of Medicine
660 South Euclid Avenue
St. Louis, Missouri 63110

Summary

NKG2D is known to trigger the natural killer (NK) cell lysis of various tumor and virally infected cells. In the NKG2D/ULBP3 complex, the structure of ULBP3 resembles the α1 and α2 domains of classical MHC molecules without a bound peptide. The lack of α3 and β2m domains is compensated by replacing two hydrophobic patches at the underside of the class I MHC-like β sheet floor with a group of hydrophilic and charged residues in ULBP3. NKG2D binds diagonally across the ULBP3 α helices, creating a complementary interface, an asymmetrical subunit orientation, and local conformational adjustments in the receptor. The interface is stabilized primarily by hydrogen bonds and hydrophobic interactions. Unlike the KIR receptors that recognize a conserved HLA region by a lock-and-key mechanism, NKG2D recognizes diverse ligands by an induced-fit mechanism.

Introduction

The activity of natural killer (NK) and myeloid cells depends on the balance of a number of activating and inhibitory receptors (Moretta et al., 2001; Long, 1999). In the past few years, much effort has been focused on characterizing the structure and function of the inhibitory NK cell receptors specific for MHC class I molecules. These receptors inhibit NK cell-mediated lysis of target cells expressing class I MHC molecules, while allowing lysis of class I-negative cells (Ljunggren and Karre, 1990). Structurally, the inhibitory receptors belong to either the immunoglobulin superfamily (IgSF) or the C-type lectin-like receptor (CTLR) superfamily. IgSF inhibitory receptors include the human killer cell Ig-like receptors (KIR), which recognize the α1 and α2 domains of human leukocyte antigens (HLA)-A, -B, and -C and the Ig-like transcripts (ILTs, also named as leukocyte Ig-like receptors or LIRs) that recognize the nonpolymorphic α3 domain of classical and nonclassical HLA molecules as well as the cytomegalovirus-encoded class I-like protein UL18 (Chapman et al., 1999). Members of the CTLR superfamily include the CD94/NKG2A that recognizes the nonclassical class I molecules HLA-E and Qa-1b in human and mouse (Lanier, 1998; Vance et al., 1998), respectively, and murine Ly-49 molecules that recognize the classical class I MHC ligands (Yokoyama, 1998). Examples of MHC recognition by KIR and Ly49 inhibitory receptors were shown in the cocrystal structures of KIR2DL2/HLA-Cw3, KIR2DL1/HLA-Cw4, and Ly49A/H2-D^d (Boyington et al., 2000a; Fan et al., 2001; Tormo et al., 1999).

In contrast to inhibitory receptors, much less is known about the structure and function of activating NK and myeloid cell receptors. Like inhibitory receptors, activating receptors are either IgSF or CTLR superfamily members. Activating IgSF receptors include 2B4, the natural cytotoxicity receptors NKp46, NKp30, and NKp44 (Moretta et al., 2001), and some activating isoforms of KIRs and ILTs/LIRs. Activating CTLR receptors include CD94/NKG2C, CD94/NKG2E, activating isoforms of Ly49, and NKG2D. All activating receptors, except 2B4, display a charged lysine or arginine residue in their transmembrane region to pair with a negatively charged adaptor molecule, such as DAP12, DAP10, CD3ζ, or FcRγ.

NKG2D is a member of CTLR superfamily and is distantly related to NKG2A, B, C, and E. When expressed on NK cells, NKG2D can trigger cytotoxicity against certain tumor cells; expression on $CD8^+$ αβ T and γδ T cells provides a costimulatory signal against virally infected cells (Bauer et al., 1999; Wu et al., 1999; Groh et al., 2001; Das et al., 2001). Efforts to search for NKG2D ligands have led to the identification of MICA and MICB in humans and Rae-1 and H60 in mice (Bauer et al., 1999; Cerwenka et al., 2000; Diefenbach et al., 2000). MICA and MICB display α1, α2, and α3 domains similar to those found in class I MHC heavy chains, but do not associate with peptides or β2-microglobulin (Li et al., 1999). Rae-1 and H60 are also class I-like molecules, but contain only the α1 and α2 domains. More recently, a group of human cytomegalovirus glycoprotein UL16 binding proteins, named ULBPs, have been identified as additional ligands to human NKG2D. Like Rae-1, ULBPs contain only α1 and α2 domains similar to those of class I MHC, do not bind peptides, and are GPI-anchored (Cosman et al., 2001). The sequence identities among MICs and ULBPs are about 25%, making NKG2D a unique activating receptor with the ability to bind diverse MHC class I-like ligands. The structural basis of such broad specificity of NKG2D is yet unknown. Recently, the crystal structures of NKG2D and its complex with MICA revealed that the receptor adopts a CD94-like structure, and its recognition of MICA shares similarity with, but is distinctly different from, the recognition of classical class I MHC molecules by T cell receptors (TCR) (Wolan et al., 2001; Li et al., 2001). Here, we report the 2.6 Å resolution structure of the extracellular domain of human NKG2D complexed with ULBP3. Comparison of this complex with previous NKG2D structures reveals

[4] Correspondence: psun@nih.gov

Table 1. Data Collection, Phasing, and Refinement Statistics

Data Collection	SeMet (remote)	SeMet (peak)	SeMet (edge)
Wavelength (Å)	0.9639	0.9792	0.9795
Resolution limit (Å)	2.7	2.6	2.7
Unique reflections	24349 (2404)[a]	26678 (2683)	24396 (2412)
Redundancy	4.4 (4.3)	5.4 (5.2)	7.1 (7.0)
Completeness (%)	99.9 (99.9)	99.7 (99.9)	99.9 (99.9)
R_{sym} (%)[b]	9.0 (43.5)	8.3 (40.0)	8.2 (37.5)
$<I/\sigma(I)>$	19.1 (3.5)	22.6 (3.9)	29.5 (5.7)
Phasing (41–2.9 Å)			
Mean figure of merit		0.59	
R_{Cullis}[c]	0.76	0.68	0.62
Phasing power[d]	1.32	1.73	1.92
Refinement			
Resolution (Å)	41–2.6		
No. reflections	14728		
No. protein atoms	3406		
No. solvent atoms	122		
R_{cryst} (%)	22.0 (38.6)		
R_{free} (%)[e]	26.8 (49.0)		
Mean B-factor (Å^2)	39		
Wilson B-factor (Å^2)	55		
Rmsd bond lengths (Å)	0.009		
Rmsd bond angles (°)	1.89		

Percentage of residues for the: most favored region, 78.7%; additional allowed region, 19.1%; generously allowed region, 2.2%; and disallowed region, 0.0% of Ramachandran plot.

[a] Values for highest resolution shells: remote, 2.8–2.7; peak, 2.7–2.6; and edge, 2.8–2.7 Å are given in parentheses.

[b] $R_{sym} = 100 \times \Sigma|I_h - <I_h>|/\Sigma I_h$, where $<I_h>$ is the mean intensity of multiple measurements of symmetry equivalent reflections.

[c] R_{Cullis} = rms(E)/rms(ΔF), where E is the phase-integrated lack of closure and ΔF is the dispersive or anomalous difference.

[d] Phasing power = rms(F_H)/rms(E), where F_H is the calculated heavy-atom structure factor.

[e] R_{free} was calculated using test set of 5%.

the molecular basis for the broad specificity of NKG2D. The crystal structure of ULBP3 provides an image of a class I-like molecule that lacks the α3 domain and is GPI-anchored to the membrane.

Results and Discussion

Overall Structure of the Complex

The structure of a human NKG2D receptor in complex with its ligand, ULBP3, has been determined by a combination of molecular replacement and multiwavelength anomalous dispersion (MAD) methods and refined to 2.6 Å resolution (Table 1). The refined (2Fo-Fc) electron density is continuous throughout the complex, except for one surface loop of ULBP3 (residues 90–97) at the C-terminal end of the α1 helix, and is away from the receptor interface. The refined R factors are 22.0% and 26.8% for R_{cryst} and R_{free}, respectively. Each crystallographic asymmetric unit contains one NKG2D dimer and one ULBP3 molecule.

The overall shape of the NKG2D/ULBP3 complex resembles a crab preying on a seashell (Figure 1A). The crab shaped receptor uses its claw shaped β strands and loops at the end opposite to both the N and C termini to grab on the ridge-shaped helical surface of ULBP3. This mode of complex formation is also observed in the NKG2D/MICA complex (Figure 3A). The relative orientation between NKG2D and ULBP3 is similar to that between KIR and HLA and that between TCR and its MHC ligands. The long axis of the receptor fits diagonally across the helical axes of ULBP3. The receptor footprint covers the C-terminal half of the α1 helix and the N-terminal half of the α3 helix of ULBP3 (Figure 1B). Both subunits of NKG2D bind ULBP3 with identical receptor loops. However, the interaction between a homodimeric NKG2D and the asymmetrical ULBP3 results in an asymmetrical receptor subunit orientation that contrasts with the perfect 2-fold symmetry observed in the ligand-free murine receptor.

The ULBP3 Structure

As predicted from its sequence, the ULBP fold consists of a set of α1/α2-like domains of MHC molecules, with two long helices situated atop an eight-stranded antiparallel β sheet (Figures 1 and 2). The same fold is also observed in the structure of MICA, with the exception that ULBP3 lacks the corresponding α3 domain of a class I MHC heavy chain (Figure 3) (Li et al., 1999). A structural comparison resulted in root-mean-square (rms) differences of 2.2 Å for 138 Cα atoms between ULBP3 and MICA and 2.5 Å for 131 Cα atoms between ULBP3 and HLA-Cw3. The conformation of the eight-stranded β sheet agrees quite well among ULBP3, MICA, and HLA-Cw3. The differences exist primarily in the loop and helical regions. All class I and II MHC molecules present peptides. An obvious question here is whether ULBP retains the peptide binding capability. No peptide has been found associating with known MHC-like proteins, such as the neonatal Fc receptor (FcRn) (Burmeister et al., 1994), hereditary haemochromatosis protein HFE (Bennett et al., 2000), and MICA (Figure 3D). Likewise, no visible electron density could be attributed to

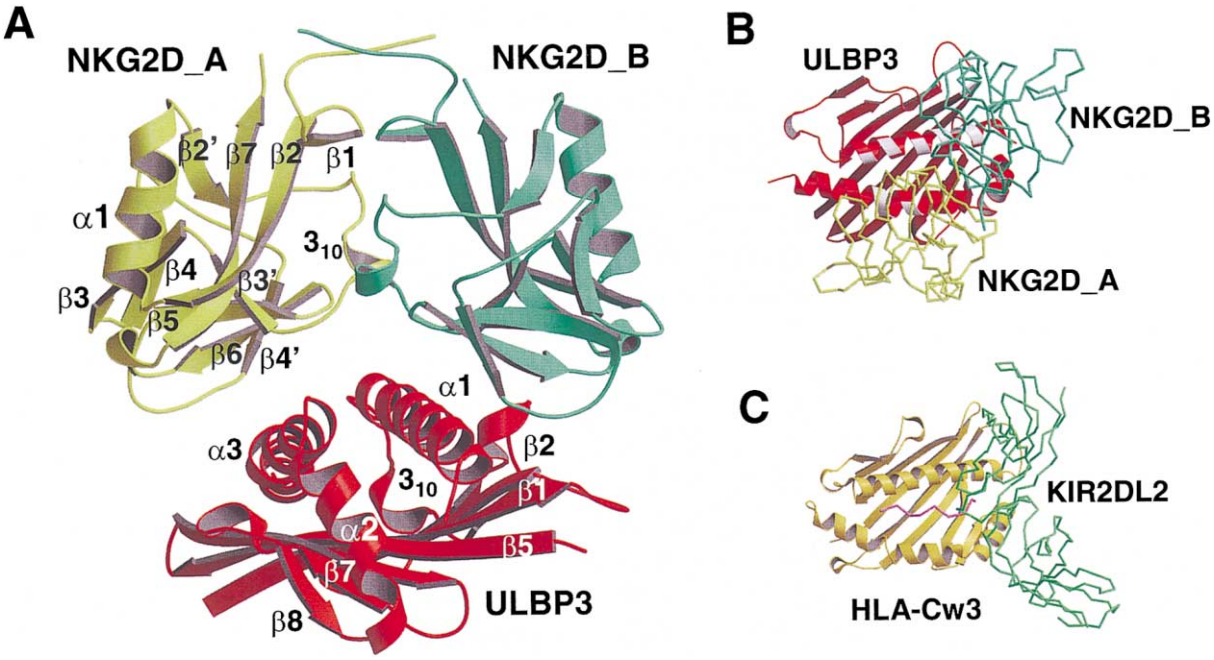

Figure 1. Ribbon Drawing of the NKG2D-ULBP3 Complex

(A) Front view. Subunits A and B of the NKG2D homodimer are shown in yellow and green, respectively. ULBP3 is colored red. All secondary structure elements on the NKG2D monomer and major ones on ULBP3 are marked in accordance with the sequence alignment in Figure 2.

(B) Top view of the NKG2D and ULBP3 complex. The color scheme is the same as in (A). ULBP3 residues in contact with the receptor are shown in white.

(C) The structure of the KIR2DL2 (green) and HLA-Cw3 (yellow) complex. The view is the same as in (B). The peptide is shown in magenta.

This figure and all subsequent ribbon drawings are prepared using the programs MOLSCRIPT (Kraulis, 1991) and RASTER3D (Merritt and Bacon, 1997).

peptides near the corresponding peptide binding region of ULBP3. The spacing between the α helices of ULBP3 ranges from 8 to 14 Å, the narrowest among all MHC homologs (Figure 3D). In comparison, the separation between the opposing α1 and α3 helices of HLA-Cw3 is 15–20 Å. The narrow groove of ULBP3 is filled with 13 hydrophobic side chains from the opposing helices (Figure 3B). In addition, a salt bridge, conserved in all three ULBP sequences, is formed between Asp 87 of the α1 helix and Lys 151 of the α2 helix, which further stabilizes the closed groove conformation.

Class I MHCs but Not ULBP3 Require α3 and β2m Domains for Their Stabilities

A distinct feature of the ULBP structure is that it lacks the homologous α3 and β2m domains of class I MHC. This appears to contradict the belief that the class I MHC fold is not stable without the α3 and β2m domains. When the underside of the eight-stranded β sheet is compared between ULBP3 and MHC structures, this region is considerably more hydrophobic in class I MHC molecules than in ULBP3. In fact, there are two hydrophobic patches located at the underside of MHC α1/α2 domains that interact with a set of hydrophobic residues from the α3 and β2m domains (Figure 3C). Most of these hydrophobic residues are conserved among class I MHC sequences. Without the α3 and β2m domains, these hydrophobic patches would be exposed to the solvent, creating stability and solubility problems. In contrast, the corresponding residues in ULBP3 (and those in the sequences of Rae-1 and H60) are mostly hydrophilic and charged residues that exist favorably when exposed to the solvent (Figure 3C). MICA also lacks the hydrophobic residues in the corresponding β2m attachment site of MHC and, thereby, exists stably without the β2m subunit. This predicts that stable α1/α2 domains can only exist in class I MHC molecules providing the hydrophobic residues in the two hydrophobic patches are mutated to hydrophilic or charged residues.

The NKG2D Structure

As a member of CTLR superfamily, NKG2D is distantly related to NKG2A, B, and C, sharing less than 30% in sequence identity. Unlike other NKG2 receptors that pair with CD94, NKG2D functions as a homodimeric receptor. The structure of NKG2D was solved by molecular replacement using a murine NKG2D as the initial model (Wolan et al., 2001). The two subunits of the NKG2D have nearly identical structures with a 0.6 Å rms deviation between 119 superimposed Cα atoms (Figure 4A). Each subunit can also be readily superimposed onto those of murine NKG2D, resulting in rms deviations of 0.7–0.9 Å with the free and MICA-complexed receptor (Figure 4B). Similar to the MICA-bound receptor, the ULBP3-bound NKG2D displays a 5° rotation between the monomers, creating an asymmetric arrangement of the receptor dimer. Only two loop regions, residues 162–164 and 183–186, deviate more than 4 Å among the three forms of

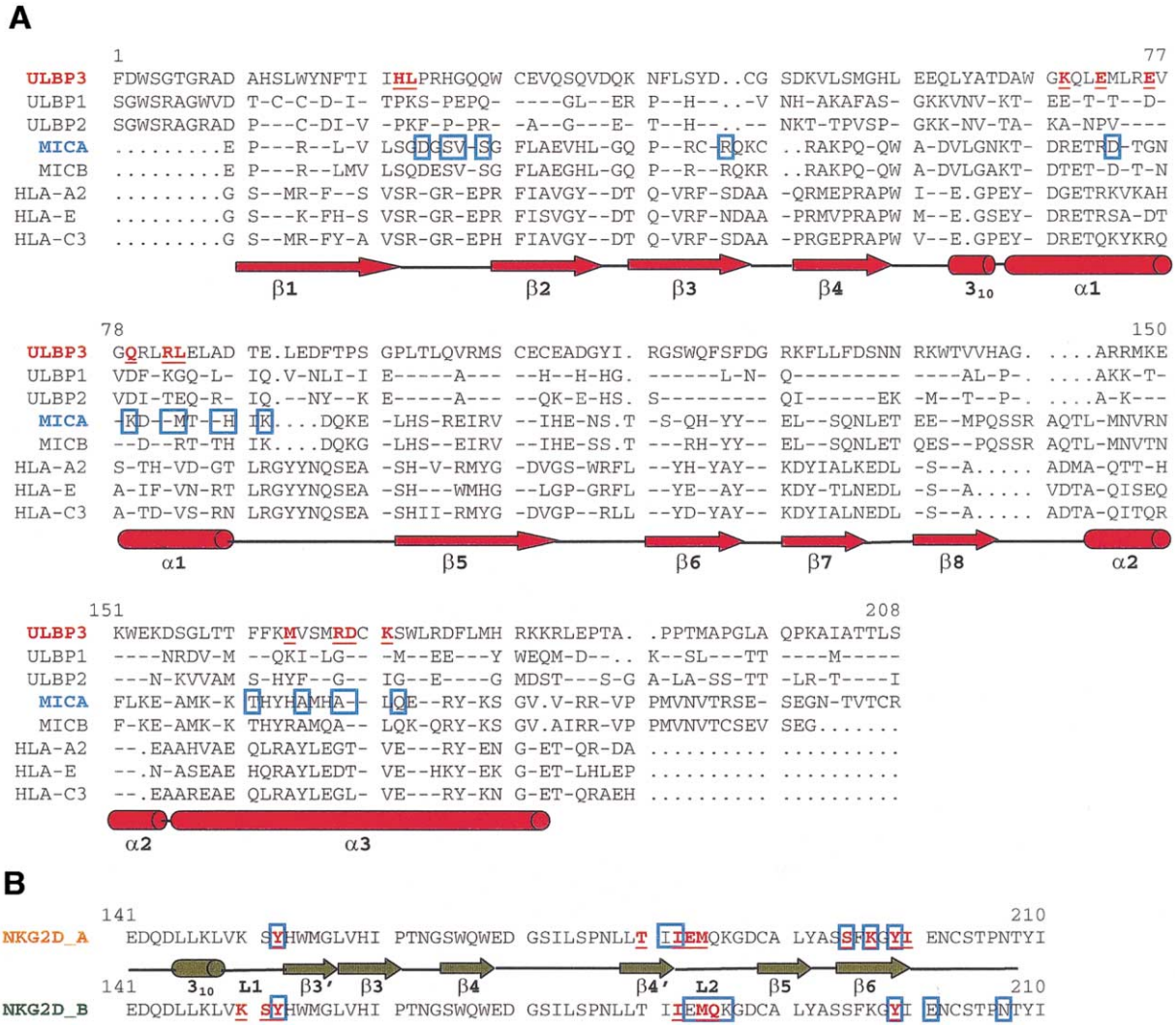

Figure 2. The Amino Acid Sequence of ULBPs and NKG2D

(A) Sequence alignment among the corresponding α1 and α2 regions of ULBP1, 2, and 3, MICA/B, HLA-A2, HLA-E, and HLA-Cw3. Residues identical to the ULBP3 sequence are represented by (-). Gaps are indicated with (.). The numbering is consistent with the mature sequence of ULBP3. The secondary structure elements of ULBP3 illustrated as arrows for β strands and cylinders for α helices are β1 (9–21), β2 (29–37), β3 (39–46), β4 (49–56), β5 (98–110), β6 (116–123), β7 (126–132), β8 (136–142), 3_{10} helix (60–64), α1 (65–87), α2 (145–155), and α3 (156–183). The ULBP3 residues interacting with NKG2D are highlighted in red and underlined. The MICA residues in contact with NKG2D, as reported in the NKG2D/MICA complex crystal structure, are boxed in blue.

(B) Regions of the NKG2D sequence, including the ULBP3 interface, are shown for both subunits with the secondary structure illustrated. Amino acids of the A and B subunits that are in contact with ULBP3 are highlighted in red and underlined, and residues that interact with MICA are boxed in blue. L1, L2, and β6 are involved in the binding of ULBP3.

NKG2D structures. The conformational difference in the first loop, residues 162–164, is most likely caused by crystal packing forces, since it is located at a crystal contact region. The second loop, residues 183–186 (L2), contacts ULBP3, and its conformation may reflect the influence of the ligand. Superpositions of NKG2D with CD94 and Ly49A resulted in rms deviations of 1.4 Å and 1.7 Å, respectively, for 97 pairs of Cα atoms (Figure 4C). The second canonical helix, common to Ly49A and other C-type lectins, is only a one-turn 3_{10} helix in the structure of NKG2D and is further deformed in CD94. Like CD94, NKG2D also lacks the appropriate Ca^{2+} ligands in its corresponding "Ca^{2+} binding loops" and thus is presumed to be a non-Ca^{2+} binding CTLR. A 25° rotation in the dimer orientation is found when the structure of NKG2D is compared with CD94. The NKG2D dimer interface is formed by the juxtaposition of the β1 strand from each monomer and by the abutting of the short 3_{10} α helices, similar to CD94 homodimer. In addition, interactions between the N termini of NKG2D (Tyr 95, Cys 96, and Pro 98) further extend the receptor dimer interface to 1850 $Å^2$, compared to 1200 $Å^2$ observed in the structure of CD94 (Boyington et al., 1999).

The Interface between NKG2D and ULBP3

The two NKG2D subunits form a concave surface in which the convex shaped ULBP3 interacts with both subunits of the receptor. The interface shape comple-

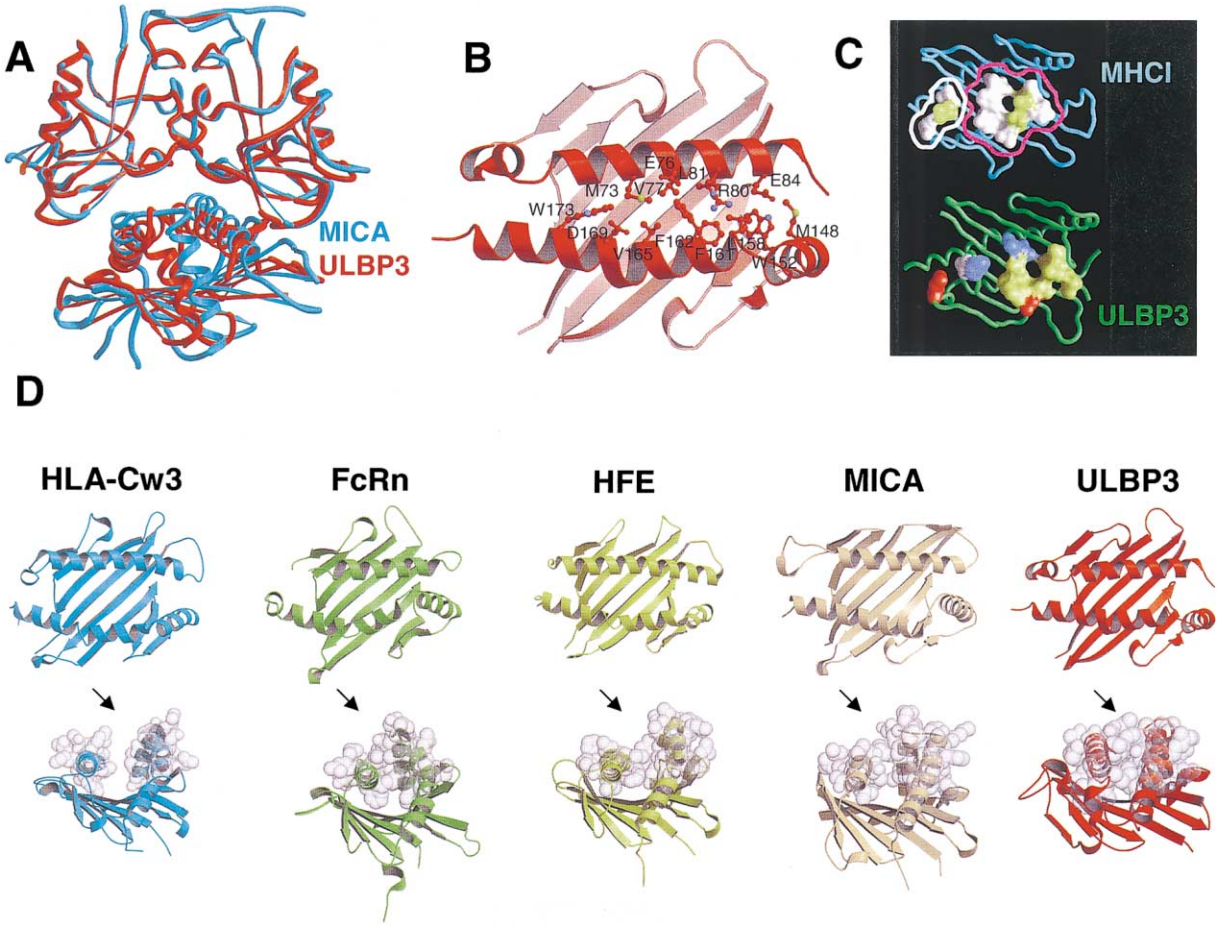

Figure 3. Structural Comparison of ULBP3 with Other Class I MHC-Related Molecules

(A) Structural overlay between the NKG2D/ULBP3 (red) and NKG2D/MICA (cyan) complexes. The complexes are superimposed at the respective NKG2D. The α3 domain of MICA is omitted for clarity. The coordinates for the NKG2D/MICA complex are taken from the Protein Data Bank entry 1hyr.

(B) Hydrophobic residues that fill the inside of the groove between the helices.

(C) Surface representation of the interface between the α1/α2 (cyan worm) domains and the α3 and β2m domains of MHC class I. Positively charged, negatively charged, polar, and hydrophobic residues are colored blue, red, yellow, and white, respectively. Areas of α1/α2 domains contacting α3 and β2m are outlined in white and magenta, respectively. For comparison, the corresponding residues of ULBP3 (green worm) are also shown with the same color scheme. This figure and Figure 5C were generated using the program GRASP (Nicholls et al., 1991).

(D) Structural comparison of the α1 and α2 domains of class I MHC with its homologs. The top panel shows the spacing of the helices in the α1 and α2 domains. The bottom panel shows the space-filling model of the putative peptide binding groove (indicated by the arrows). The groove is partially closed in the structures of FcRn, HFE, and MICA and completely disappears in ULBP3. The Protein Data Bank entries are 1efx, 1exu, 1de4, and 1b3j for HLA-Cw3, FcRn, HFE, and MICA, respectively.

mentarity value Sc is 0.65 between the receptor and ULBP3 (Lawrence and Colman, 1993), similar to that between antibodies and antigens (Ysern et al., 1998), greater than those between KIR and HLA or between TCR and MHC (Sc = 0.5–0.6) (Boyington et al., 2000a), but smaller than the value of 0.72 between NKG2D and MICA (Li et al., 2001). This indicates a good surface complementarity at the receptor-ligand interface. The total buried interface is 1930 Å^2 (8.2% and 10.7% of the respective NKG2D and ULBP3 surfaces), slightly smaller than the 2180 Å^2 buried between NKG2D and MICA (Li et al., 2001), but larger than the 1560 Å^2 interface between KIR and HLA (Boyington et al., 2000a) or the 1700–1800 Å^2 between TCR and MHC (Garboczi et al., 1996; Garcia et al., 1996; Reinherz et al., 1999). Each receptor subunit contributes approximately half of the total interface area. In all, six receptor segments, three similar segments from each subunit, interact with the ligand (Figure 2B). They are loop L1, residues 150–152; loop L2, residues 180–186 (also referred as the Ca^{2+} binding region in a classical C-type lectin); and strand β6. The receptor-ligand interface is stabilized primarily by a network of hydrogen bonds and hydrophobic interactions (Figure 5; Table 2). There are ten hydrogen bonds throughout the interface area; subunit A contributes six and subunit B contributes four (Figure 5A; Table 2). Each NKG2D subunit forms a hydrophobic patch with ULBP3, using the same receptor residues (Tyr 152, Ile 182, Met 184 and Tyr 199), but different ligand residues (Figure 5B). The hydrophobic patch within subunit A contacts Met 164 and Arg 168 (the aliphatic region) of ULBP3, whereas the patch within subunit B interacts with Gln

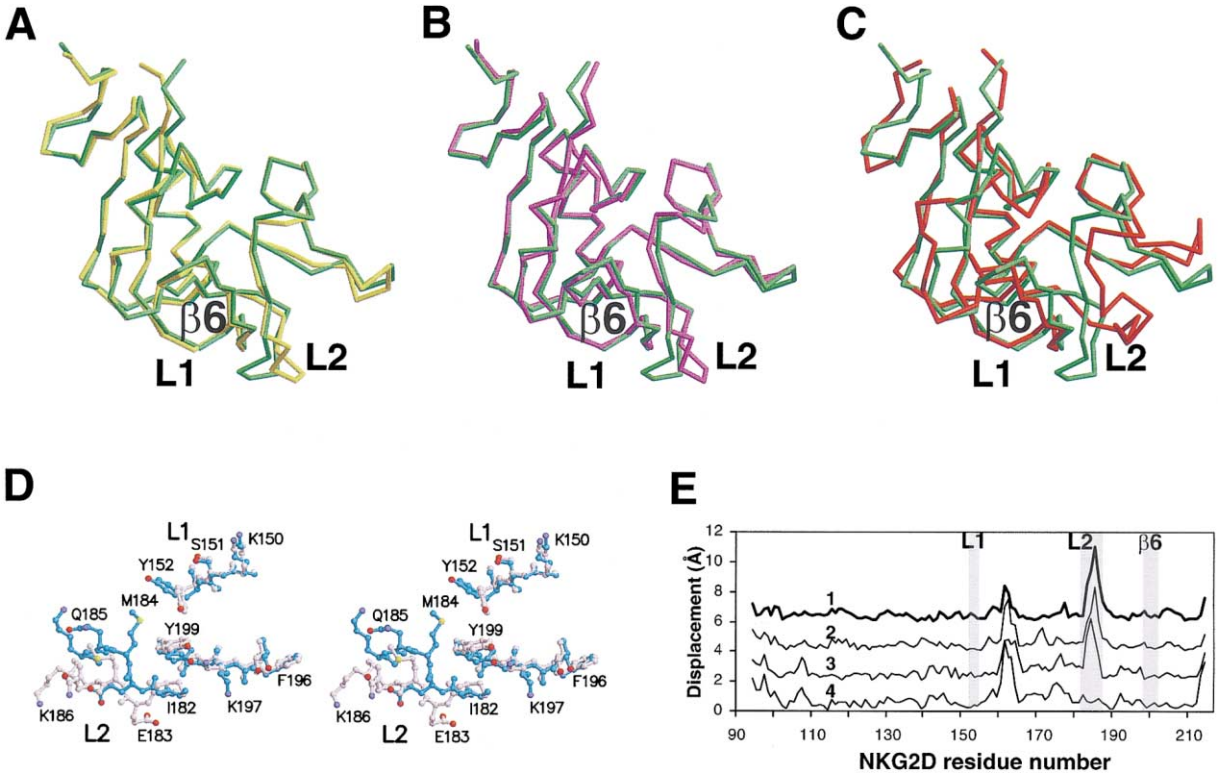

Figure 4. Structural Comparisons between the NKG2 Family of C-Type Lectin Receptors

Superpositions are shown between the structures of (A) subunit A (yellow) and B (green) of the ULBP-bound NKG2D; (B) subunit B (green) of the current NKG2D and ligand-free receptor (magenta); and (C) the subunit B (green) of the current NKG2D and CD94 monomer (red). The coordinates for the free NKG2D and CD94 receptors are from the Protein Data Bank entries 1hq8 and 1b6e, respectively. (D) Stereo view of a structrual comparison between the ULBP3 binding loops in the A (white) and B (cyan) subunits of NKG2D. Tyr 152 in loop L1 displays different side chain rotamer conformation in A and B subunits. L2 loops in the two subunits display the largest conformational changes. Strand β6 has the same conformation in both subunits. (E) Structural comparison among the known NKG2D structures shown as the displacement in the Cα atoms. Curves 1, 2, 3, and 4 are the calculated differences in Cα positions between the current NKG2D A and B subunits; the current subunit A and that from the MICA complex; the current subunit B and the ligand-free NKG2D structure; and the current subunit A and the ligand-free NKG2D structure, respectively. The two MICA-bound NKG2D subunits display a similar L2 loop conformation that is different from the ligand-free NKG2D. Curves 1, 2, and 3 are shifted along the vertical axis for clarity. Shaded regions indicate the ULBP binding loops, L1, L2, and strand β6. Large structural displacement indicates main chain conformational changes.

79, Leu 83, Ala 86, and Arg 82 (the aliphatic region) of ULBP3. Two salt bridges are formed at the interface, one between Lys 197 of subunit A and Asp 169 of ULBP3 and the other between Lys 150 of subunit B and Glu 76 of the ULBP. There are, however, unbalanced charges at the interface. For example, Lys 150 of NKG2D subunit A is in close contact (4.2 Å) with Arg 80 of the ULBP with no counter charges nearby, creating an unfavorable electrostatic interaction. The lack of an overall charge complementarity implies that charge-charge interactions play a secondary role in the receptor-ligand recognition (Figure 5C).

Conformational Plasticity in NKG2D/ULBP3 Recognition

Conformational plasticity or induced-fit binding refers to a situation where a receptor undergoes ligand-specific conformational adjustments upon complex formation. This is opposed to lock-and-key recognition, where no conformational adjustment takes place upon complex formation. Both induced-fit and lock-and-key modes of recognition have been observed in various receptor-ligand systems. Many cytokine signalings are thought to involve induced-fit mechanisms, as observed in the structures of hematopoietic cytokines and their receptor complexes and as demonstrated by mutational studies on the growth hormone receptor (de Vos et al., 1992; Atwell et al., 1997; Livnah et al., 1996). Certain T cell receptor and class I MHC complexes (Garcia et al., 1998), IgE-Fc and FcεRI complexes (Garman et al., 2000), and antigen-antibody complexes are also examples of induced-fit recognitions. In contrast, the KIR/HLA complex, IgG-Fc/FcγRIII receptor complex, and adhesion CD2/CD58 complex are examples of the lock-and-key type of recognition (Boyington et al., 2000a; Radaev et al., 2001; Wang et al., 1999).

The NKG2D/ULBP3 complex displays characteristic features of an induced-fit recognition. First, binding to ULBP resulted in an asymmetric orientation of the homodimeric NKG2D subunits. A similar adjustment in the receptor subunits was also observed in the NKG2D/MICA complex structure (Li et al., 2001). In addition, local conformational changes are also observed in the three NKG2D elements that contact the ULBP. Specifi-

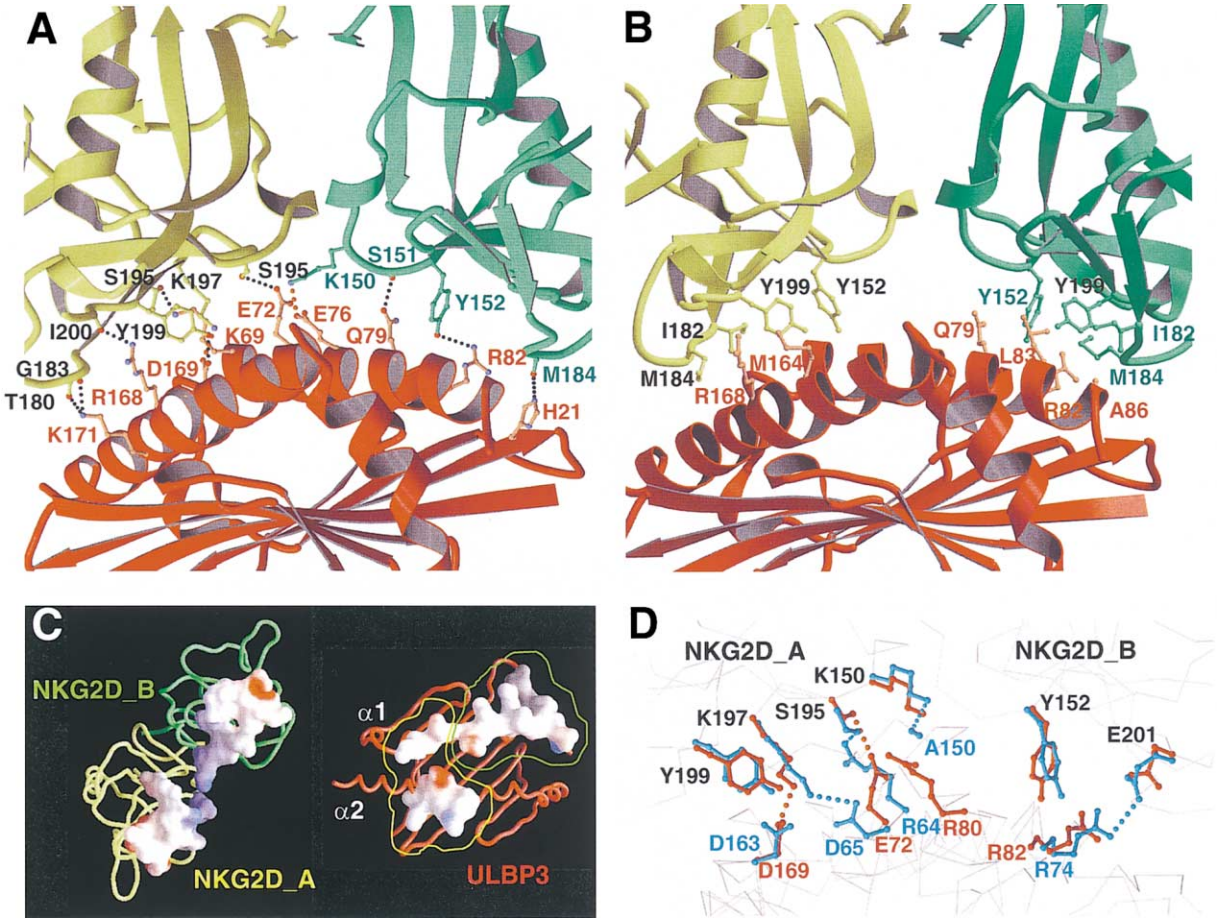

Figure 5. Interface Residues between NKG2D and ULBP3

(A) Residues involved in hydrogen bonds (black dotted lines) and salt bridges (red dotted lines). NKG2D is colored in yellow and green for A and B subunits, respectively. ULBP3 is colored in red. Residues are colored according to their chain color. The view is similar to the front view of Figure 1A.

(B) Residues involved in hydrophobic interface patches. The color scheme is the same as in (A). Tyr 152, Ile 182, Met 184, and Tyr 199 from NKG2D subunit A form a hydrophobic patch with Met 164 and Arg 168 from the α3 helix of ULBP3. The same residues from subunit B form a hydrophobic patch with Gln 79, Arg 82, Leu 83, and Ala 86 from the α1 helix of ULBP3.

(C) Surface representation of the NKG2D/ULBP3 interface colored according to electrostatic potential distribution, with positive charges in blue and negative charges in red. Patches of ULBP3 in contact with A and B subunits of NKG2D are outlined in yellow and green, respectively.

(D) Conformational plasticity involved in the recognition of ULBP and MICA by NKG2D. Side chains in the NKG2D/ULBP3 complex and the NKG2D/MICA complex are shown in red and cyan, respectively. Only those hydrogen bonds and salt bridges that are different between the two complexes are presented as red and cyan dotted lines for NKG2D/ULBP3 and NKG2D/MICA, respectively. In both the NKG2D/ULBP3 and the NKG2D/MICA structures, Tyr 199 of NKG2D subunit A forms a hydrogen bond with Asp 169 (Asp 163 in MICA). However, in the complex with ULBP3, Asp 169 (ULBP3) also forms a salt bridge with Lys 197 of the NKG2D subunit, whereas the same Lys 197 from the MICA-bound receptor makes a salt bridge with Asp 65 (MICA). In the ULBP3 complex, Ser 195 of NKG2D subunit A forms a hydrogen bond with Glu 72, whereas the same residue in the MICA complex is bound to Arg 64. In the MICA complex, Lys 150 of NKG2D subunit A forms a hydrogen bond with the carbonyl oxygen of Ala 150, whereas in the ULBP3 complex, the same lysine makes no hydrogen bonds and is in close contact with Arg 80 of ULBP3. In both the ULBP3 and MICA complexes, Tyr 152 of NKG2D subunit B makes hydrogen bonds with Arg 82 (Arg 74 in MICA). However, in the MICA complex, Arg 74 forms a salt bridge with Glu 201 of NKG2D, whereas in the ULBP3 complex, Glu 201 is located 4.5 Å apart from Arg 82.

cally, the L2 loop from the A subunit displays the same conformation as in the ligand-free receptor (Figure 4E, curve 4), whereas the same loop in the B subunit adopts an alternative conformation that is also represented in the structure of the MICA-bound NKG2D (Figures 4D and 4E, curves 1, 3, and 4). Residues of the L1 loop and β6 strand, such as Lys 197 and Tyr 152, adopt unique side chain conformations in each subunit, resulting in different hydrogen bond and salt bridge formations upon complex formation (Figure 4D). Second, different receptor residues were recruited from each subunit to match the asymmetric ULBP3 surfaces. Although both subunits of NKG2D employ loops L1 and L2 and β6 strand to bind ULBP3, about half of the interface residues vary between the subunits as a result of interacting with different ULBP3 residues (Figure 2B; Table 2). The ability of NKG2D to recruit different residues to match similar but distinct ligand surfaces is best exemplified by comparing the NKG2D/ULBP3 structure with NKG2D/MICA structure. MICs and ULBPs have similar structures

Table 2. Interface Contacts between NKG2D and ULBP3

NKG2D	Chain ID	ULBP3	Distance (Å)
Hydrogen bonds and salt bridges			
Thr 180 $O_{\gamma 1}$	A	Lys 69 N_{ζ}	2.6
Glu 183 O	A	Lys 171 N_{ζ}	2.7
Met 184 O	A	Lys 171 N_{ζ}	2.9
Ser 195 O_{γ}	A	Glu 72 $O_{\epsilon 2}$	3.0
Lys 197 N_{ζ}	A	Asp 169 $O_{\delta 2}$	2.7
Tyr 199 OH	A	Asp 169 $O_{\delta 2}$	2.4
Ile 200 O	A	Arg 168 NH1	2.8
Lys 150 N_{ζ}	B	Glu 76 $O_{\epsilon 2}$	2.7
Lys 150 N_{ζ}	B	Glu 76 $O_{\epsilon 1}$	3.4
Ser 151 O_{γ}	B	Gln 79 $O_{\epsilon 1}$	2.7
Glu 183 O	B	His 21 $N_{\epsilon 2}$	3.4
Tyr 152 OH	B	Arg 82 NH2	3.1
Met 184 O	B	His 21 $N_{\epsilon 2}$	3.4
Hydrophobic contacts[a]			
Tyr 152	A	Met 164	
Ile 182	A	Arg 168	
Met 184	A	Arg 168	
Tyr 199	A	Met 164, Arg 168	
Lys 150	B	Glu 76	
Tyr 152	B	Gln 79, Leu 83	
Ile 182	B	Ala 86, Asp 87	
Met 184	B	His 21, Arg 82, Ala 86	
Gln 185	B	Pro 23	
Ala 193	B	Leu 83	
Tyr 199	B	Leu 83	

[a] The list of contacts < 4.0 Å.

but share only 25% sequence identity. Despite an overall similarity in the receptor docking between MICA and ULBP3, the detailed receptor-ligand interactions are quite different. For example, Ser 195 of NKG2D forms a hydrogen bond with Glu 72 of ULBP3, but the same Ser interacts with Arg 64 of MICA. Among the 12 ULBP3 residues that contact NKG2D, only two, Arg 82 and Asp 169, are conserved in MICA (Figures 2A and 5D). However, they do not mediate the same interface contacts. While Asp 169 of ULBP3 forms a salt bridge with Lys 197 of NKG2D, the equivalent Asp in MICA is too distant (4.7 Å) from Lys 197 to form a salt bridge. Instead, Lys 197 forms a salt bridge with Asp 65 of MICA, which has no counterpart in ULBP3 (Figure 5D). It appears that the interface is less preserved than the overall sequence conservation between MICA and ULBP3. It should be noted, however, that the interface residues of ULBP3 and MICA are derived from the corresponding secondary structure elements; i.e., they share common hot spots for the receptor binding (Figures 1B and 2A). Similarly, on the receptor side, overlapping but distinct residues of NKG2D are used to bind both ULBP3 and MICA (Figure 2B). This receptor conformational plasticity in both the domain and the side chain orientations enables the receptor to adapt various ligand surfaces while preserving an overall receptor-ligand docking orientation.

To date, there are three known ULBP molecules, sharing 55%–60% sequence identity (Cosman et al., 2001). All have been shown to be ligands of NKG2D. However, only 1 of the 12 ULBP3 interface residues, Asp 169, which forms a salt bridge with Lys 197 of NKG2D, is conserved among the three ULBP sequences (Figure 2A). Again, the interface residues appear to be less conserved than the overall sequence identity among the ULBPs. It is predicted that NKG2D recognizes ULBP1 and ULBP2 through induced-fit mechanisms in a similar orientation as that of ULBP3.

Comparison of the Plastic Recognition between NKG2D/ULBP3 and TCR/HLA

The observed plastic recognition in the NKG2D/ULBP3 complex is not unprecedented. A similar situation has been observed in the structures of $\alpha\beta$ T cell receptor and class I MHC complexes. T cell receptors are, in general, restricted to particular MHC and peptide complexes. There are often multiple clones of T lymphocytes that recognize the same MHC-peptide complex. For example, both the human A6 TCR and B7 TCR, which contain different Vα segments, recognize the same HLA-A2 presenting the HTLV-1 Tax peptide. The crystal structures of both A6 TCR and B7 TCR in complex with the same HLA-peptide ligand have been determined (Garboczi et al., 1996; Ding et al., 1998). Comparison of the two TCR/HLA complexes showed that both TCRs bound to HLA-A2 in similar location and orientations. The detailed interface, however, is quite different between the two TCR/HLA complexes. Among the 17 HLA contact residues of B7 TCR, 16 are different from those observed in the A6 TCR/HLA-A2 complex. Moreover, the two receptors contact a set of overlapping but distinct HLA-A2 residues. The differences in the interface amino acids were accommodated by minor conformational changes in the CDR loops of the TCR Vα and Vβ chains, such that both receptors recognize the same HLA-A2 in a similar orientation. Conformational plasticity was also observed in the murine 2C TCR and H-2k^{d} complex (Garcia et al.,

1998). The observation of plastic interfaces in both the NKG2D/ULBP3 and NKG2D/MICA complexes suggests that NKG2D uses an induced-fit rather than lock-and-key mechanism to achieve its specificity for multiple ligands. It is possible that induced-fit occurs as a general mechanism for receptors to recognize diverse ligands.

A Model for CD94/NKG2A Recognition of HLA-E

It is anticipated that the overall docking between CD94/NKG2 receptors and HLA-E resembles that between NKG2D and ULBP3, owing to the structural similarities in both the receptors and the ligands (O'Callaghan et al., 1998; Boyington et al., 1999). A model for a complex between CD94/NKG2 and HLA-E can be generated in which the peptide of HLA-E, specifically the Arg at the P5 position, forms a hydrogen bond with a Ser residue on the respective L1 loop of NKG2A.

Implications for the Activating and Inhibitory NK Receptor Functions

In contrast to the adapted immune receptors, such as antibodies and TCR, which rely on gene recombination and somatic mutations to give rise diverse ligand specificities, innate immune receptors are germline coded and lack the flexibility to adapt multiple ligands at gene level. Two distinct mechanisms appear to have evolved for the activating and inhibitory NK receptors to overcome their ligand diversities. NKG2D, an example of the activating receptors, uses induced-fit mechanisms to recognize ligands with less than 20% sequence conservation. Functionally, the activating receptor NKG2D recognizes tumor or viral infections by alerting molecules such as MICs and ULBPs. The polymorphism and sequence diversity observed in MIC and ULBP presumably reflect the diversity of pathogens. Through induced-fit mechanisms, the receptor acquires the ability to bind multiple ligands with little sequence conservation. For example, the human cytomegalovirus-encoded protein UL16 binds to ULBP1, ULBP2, and MICB, but not to ULBP3 or MICA (Cosman et al., 2001). One possible function of UL16 is to block immune recognition of the virus-infected cells by binding and interfering with the ligand recognition of NKG2D. The ability to recognize multiple ligands or highly polymorphic ligands provides a means for NKG2D to circumvent the viral blockade of a particular NKG2D/ligand interaction. In contrast, the structures of inhibitory KIR/HLA complexes showed little or no conformational changes upon ligand recognition (Boyington et al., 2000a; Fan et al., 2001), indicating a lock-and-key or rigid body recognition between the KIR and HLA. Among the multiple class I MHC ligands of KIR, the interface residues, contrary to those of the NKG2D ligands, are over 90% conserved. Functionally, the inhibitory receptors recognize primarily self-molecules on normal cells. Alteration of self constitutes a necessary and sufficient signal of danger and leads to the release of inhibition. Since a self entity rarely changes, the inhibitory receptors, therefore, can and must be very specific for self-molecules and less tolerant to mutations. Single amino acid mutations in KIR receptors have been known to result in nearly complete loss of ligand binding and loss of protection against killing (Boyington et al., 2000a; Zappacosta et al., 1997; Peruzzi et al., 1996), suggesting that KIR/HLA recognition is sensitive to interface mutations or less tolerant to sequence changes. A lock-and-key recognition would ensure less tolerance to mutations, thus preventing the inhibitory KIR receptors from recognizing altered self.

It is tempting to speculate that the receptor-ligand binding affinities also reflect their functional needs. For example, KIR/HLA interactions were characterized with a K_D of 10–30 μM (Boyington et al., 2000a; Maenaka et al., 1999), whereas the K_D for NKG2D/MICA binding was about 1 μM (Li et al., 2001). It is conceivable that the higher ligand affinity of NKG2D permits recognition of variant ligand forms and provides the basis for mutational tolerance. Alternatively, it is advantageous for the self-recognizing inhibitory receptors to have a lower ligand binding affinity to be less tolerant to mutations.

In conclusion, the activating receptor NKG2D recognizes nonconserved regions of both ULBP3 and MICA using an induced-fit mechanism. First, NKG2D recognizes multiple ligands of diverse amino acid sequences, as evident from the lack of sequence conservation at the interface. Second, the receptor uses topologically similar but distinct sets of interface residues to counter the structural variation in ULBP3 and MICA. Finally, identical residues on the two NKG2D subunits mediate different interactions with ULBP3, leading to conformational adjustment of the interface residues. Although the structure of the NKG2D/ULBP3 complex offers considerable insight into the function of this triggering receptor, many questions regarding the receptor-ligand recognition remain to be answered. For example, it is still not clear what structural themes are shared among the diverse ligands to qualify them as the ligands of NKG2D. Namely, what are the criteria for receptor-ligand recognition? Will recognition be more tolerant of interface mutations, as suggested from the structural results? Finally, does the receptor aggregate upon ligand binding, and, if so, what is the synaptic structure of NKG2D? Space group symmetry precludes the formation of an oligomeric state in the current crystal that would be consistent with what might form in the synapse. This, however, does not rule out the possibility that NKG2D forms large molecular aggregates in the presence of coreceptors and adhesion molecules.

Experimental Procedures

Protein Expression, Purification, and Crystallization

The extracellular parts of human NKG2D receptor (residues 75–216) and ULBP3 (residues 1–200 with a His_6 tag) were both expressed in *Escherichia coli* as inclusion bodies and then reconstituted in vitro. In brief, cells containing NKG2D- or ULBP3-expressing plasmid were grown at 37°C in 10 l of LB (Luria-Bertani) broth using a Newbrunswick Bioflo 3000 Bioreactor vessel and were induced with 0.5 mM IPTG at an approximate OD_{596} of 1.7 for 4 hr. The inclusion bodies were isolated by repeated washes with 2 M urea solution and then redissolved in 6 N guanidine hydrochloride prior to refolding. The refolding was initiated by a quick dilution of dissolved inclusion bodies into a refolding buffer consisting of 0.5 M L-arginine, 2.5 mM cystamine (or oxidized glutathione), 5 mM cysteamine (or reduced glutathione), 10 μg/ml AEBSF (4-2[-aminoethyl]-benzenesulfonyl fluoride hydrochloride), and 100 mM Tris (pH 8.0) and then dialyzed thoroughly against water (Boyington et al., 2000b). The renaturated NKG2D was concentrated on a Source Q column (Amersham Pharmacia Biotech), and the renatured ULBP3 was concentrated on a Ni-NTA affinity column (Qiagen). Both proteins were

further purified on a Superdex 200 size-exclusion column (Amersham Pharmacia Biotech). The refolded products were analyzed by both N-terminal amino acid sequencing and electrospray ionization mass spectrometry (ESI-MS). The selenomethionine (SeMet) derivative of ULBP3 was prepared using a growth condition in which the bacterial methionine biosynthetic pathway was inhibited (Van Duyne et al., 1993). In brief, 40 mls of bacteria inoculum containing the ULBP expression plasmid were grown at 37°C in LB broth overnight. The LB broth in the overnight inoculum was replaced with M9 medium supplemented with 0.4% glucose, 0.1 mM $CaCl_2$, and 3 mM $MgSO_4$ and added to four 1 l shaker flasks at 37°C. The bacterial cell culture was induced at an OD_{596} of ~0.6 with 0.5 mM IPTG for 12 hr together with added (50 mg/l each) amino acids Leu, Ile, Val and (100 mg/l each) Thr, Lys, Phe, and SeMet. The refolding of the SeMet-modified ULBP was the same as for the native protein. The presence of nine SeMet residues was confirmed by ESI-MS.

The complex of NKG2D and ULBP3 was prepared by mixing both components in a 1:1 molar ratio and concentrating to 8–15 mg/ml for crystallization. Single crystals were obtained by vapor diffusion in hanging drops at room temperature from 10% PEG 3350-8000 and 50 mM MES (pH 6.0). They appeared after 1–3 days and grew to an average size of 0.1 × 0.1 × 0.05 mm in ~2 weeks.

Structure Determination

After a brief soaking in precipitant solutions containing 25% glycerol, crystals were flash frozen at 100 K. X-ray diffraction data from single crystals were collected using an ADSC Quantum IV CCD detector at the X9B beam line of the National Synchrotron Light Source (NSLS), Brookhaven National Laboratory and processed with HKL2000 (Otwinowski and Minor, 1997). The crystals belong to a space group $P4_32_12$ with cell dimensions $a = b = 62.05$ and $c = 237.3$ Å, contain one dimer of NKG2D and one ULBP3 per asymmetric unit, and diffract to 2.6 Å.

The NKG2D homodimer (PDB accession number 1HQ8) was used as a model to localize the receptor in the complex by molecular replecement using AmoRe (Navaza, 1994). The NKG2D phased density map was insufficient to localize ULBP3. A SeMet MAD dataset was collected from the crystals containing SeMet-ULBP3 at the X9B beamline (NSLS). Six selenomethionines were found in the difference electron density map with phases from NKG2D using program CNS, version 1.0 (Brunger et al., 1998). After density modification, including solvent flipping, the electron density of ULBP3 was traced unambiguously. Model adjustments and rebuilding were done using program O (Kleywegt and Jones, 1996). The positional and individual *B* factor refinement was carried out using a maximum likelihood target function of CNS v1.0. The refined model consists of residues 94–215 from NKG2D and 9–186 from ULBP3 with one loop of ULBP3, residues 90–97, missing. A well-defined glutathione molecule forms a disulfide bond to Cys 109 of ULBP3. Surface areas were calculated with the program SURFACE of the CCP4 program suite and a probe radius of 1.4 Å (CCP4, 1994). Surface complementarity was calculated with the program SC (Lawrence and Colman, 1993). Domain angles were calculated with the program HINGE (Snyder et al., 1999).

Acknowledgments

We thank C. Hammer for mass spectroscopy measurements; J. Johnson and Z. Dauter for help with X-ray synchrotron data collection; and J. Boyington and J. Briones for inclusion body preparations. This work is supported by intramural research funding from the National Institute of Allergy and Infectious Diseases. A.B. is supported by an RD Wright Fellowship from the National Health and Medical Research Council, Australia.

Received June 28, 2001; revised October 25, 2001.

References

Atwell, S., Ultsch, M., de Vos, A.M., and Wells, J.A. (1997). Structural plasticity in a remodeled protein-protein interface. Science *278*, 1125–1128.

Bauer, S., Groh, V., Wu, J., Steinle, A., Phillips, J.H., Lanier, L.L., and Spies, T. (1999). Activation of NK cells and T cells by NKG2D, a receptor for stress-inducible MICA. Science *285*, 727–729.

Bennett, M.J., Lebron, J.A., and Bjorkman, P.J. (2000). Crystal structure of the hereditary haemochromatosis protein HFE complexed with transferrin receptor. Nature *403*, 46–53.

Boyington, J.C., Riaz, A.N., Patamawenu, A., Coligan, J.E., Brooks, A.G., and Sun, P.D. (1999). Structure of CD94 reveals a novel C-type lectin fold: implications for the NK cell-associated CD94/NKG2 receptors. Immunity *10*, 75–82.

Boyington, J.C., Motyka, S.A., Schuck, P., Brooks, A.G., and Sun, P.D. (2000a). Crystal structure of an NK cell immunoglobulin-like receptor in complex with its class I MHC ligand. Nature *405*, 537–543.

Boyington, J.C., Raiz, A.N., Brooks, A.G., Patamawenu, A., and Sun, P.D. (2000b). Reconstitution of bacterial expressed human CD94: the importance of the stem region for dimer formation. Protein Expr. Purif. *18*, 235–241.

Brunger, A.T., Adams, P.D., Clore, G.M., Delano, W.L., Gros, P., Grosse-Kunstleve, R.W., Jiang, J.-S., Kuszewski, J., Nilges, N., Pannu, N.S., et al. (1998). Crystallography & NMR system: a new software suite for macromolecular structure determination. Acta Crystallogr. D Biol. Crystallogr. *D54*, 905–921.

Burmeister, W.P., Gastinel, L.N., Simister, N.E., Blum, M.L., and Bjorkman, P.J. (1994). Crystal structure at 2.2 A resolution of the MHC-related neonatal Fc receptor. Nature *372*, 336–343.

CCP4 (Collaborative Computational Project 4) (1994). The CCP4 suite: programs for protein crystallography. Acta Crystallogr. D *50*, 760–763.

Cerwenka, A., Bakker, A.B., McClanahan, T., Wagner, J., Wu, J., Phillips, J.H., and Lanier, L.L. (2000). Retinoic acid early inducible genes define a ligand family for the activating NKG2D receptor in mice. Immunity *12*, 721–727.

Chapman, T.L., Heikeman, A.P., and Bjorkman, P.J. (1999). The inhibitory receptor LIR-1 uses a common binding interaction to recognize class I MHC molecules and the viral homolog UL18. Immunity *11*, 603–613.

Cosman, D., Mullberg, J., Sutherland, C.L., Chin, W., Armitage, R., Fanslow, W., Kubin, M., and Chalupny, N.J. (2001). ULBPs, novel MHC class I-related molecules, bind to CMV glycoprotein UL16 and stimulate NK cytotoxicity through the NKG2D receptor. Immunity *14*, 123–133.

Das, H., Groh, V., Kuijl, C., Sugita, M., Morita, C.T., Spies, T., and Bukowski, J.F. (2001). MICA engagement by human Vgamma2Vdelta2 T cells enhances their antigen-dependent effector function. Immunity *15*, 83–93.

de Vos, A.M., Ultsch, M., and Kossiakoff, A.A. (1992). Human growth hormone and extracellular domain of its receptor: crystal structure of the complex. Science *255*, 306–312.

Diefenbach, A., Jamieson, A.M., Liu, S.D., Shastri, N., and Raulet, D.H. (2000). Ligands for the murine NKG2D receptor: expression by tumor cells and activation of NK cells and macrophages. Nat. Immunol. *1*, 119–126.

Ding, Y.H., Smith, K.J., Garboczi, D.N., Utz, U., Biddison, W.E., and Wiley, D.C. (1998). Two human T cell receptors bind in a similar diagonal mode to the HLA- A2/Tax peptide complex using different TCR amino acids. Immunity *8*, 403–411.

Fan, Q.R., Long, E.O., and Wiley, D.C. (2001). Crystal structure of the human natural killer cell inhibitory receptor KIR2DL1-HLA-Cw4 complex. Nat. Immunol. *2*, 452–460.

Garboczi, D.N., Ghosh, P., Utz, U., Fan, Q.R., Biddison, W.E., and Wiley, D.C. (1996). Structure of the complex between human T-cell receptor, viral peptide and HLA-A2. Nature *384*, 134–141.

Garcia, K.C., Degano, M., Stanfield, R.L., Brunmark, A., Jackson, M.R., Peterson, P.A., Teyton, L., and Wilson, I.A. (1996). An alphabeta T cell receptor structure at 2.5 A and its orientation in the TCR-MHC complex. Science *274*, 209–219.

Garcia, K.C., Degano, M., Pease, L.R., Huang, M., Peterson, P.A., Teyton, L., and Wilson, I.A. (1998). Structural basis of plasticity in T cell receptor recognition of a self peptide-MHC antigen. Science *279*, 1166–1172.

Garman, S.C., Wurzburg, B.A., Tarchevskaya, S.S., Kinet, J.P., and Jardetzky, T.S. (2000). Structure of the Fc fragment of human IgE

bound to its high-affinity receptor Fc epsilonRI alpha. Nature *406*, 259–266.

Groh, V., Rhinehart, R., Randolph-Habecker, J., Topp, M.S., Riddell, S.R., and Spies, T. (2001). Costimulation of CD8 alphabeta T cells by NKG2D via engagement by MIC induced on virus-infected cells. Nat. Immunol. *2*, 255–260.

Kleywegt, G.J., and Jones, T.A. (1996). Efficient rebuilding of protein structures. Acta Crystallogr. D Biol. Crystallogr. *52*, 829–832.

Kraulis, P. (1991). MOLSCRIPT: a program to produce both detailed and schematic plots of protein structures. J. Appl. Crystallogr. *24*, 946–950.

Lanier, L.L. (1998). NK cell receptors. Annu. Rev. Immunol. *16*, 359–393.

Lawrence, M.C., and Colman, P.M. (1993). Shape complementarity at protein/protein interfaces. J. Mol. Biol. *234*, 946–950.

Li, P., Willie, S.T., Bauer, S., Morris, D.L., Spies, T., and Strong, R.K. (1999). Crystal structure of the MHC class I homolog MIC-A, a gammadelta T cell ligand. Immunity *10*, 577–584.

Li, P., Morris, D.L., Willcox, B.E., Steinle, A., Spies, T., and Strong, R.K. (2001). Complex structure of the activating immunoreceptor NKG2D and its MHC class I-like ligand MICA. Nat. Immunol. *2*, 443–451.

Livnah, O., Stura, E.A., Johnson, D.L., Middleton, S.A., Mulcahy, L.S., Wrighton, N.C., Dower, W.J., Jolliffe, L.K., and Wilson, I.A. (1996). Functional mimicry of a protein hormone by a peptide agonist: the EPO receptor complex at 2.8 A. Science *273*, 464–471.

Ljunggren, H.G., and Karre, K. (1990). In search of the 'missing self': MHC molecules and NK cell recognition. Immunol. Today *11*, 237–244.

Long, E.O. (1999). Regulation of immune responses through inhibitory receptors. Annu. Rev. Immunol. *17*, 875–904.

Maenaka, K., Juji, T., Nakayama, T., Wyer, J.R., Gao, G.F., Maenaka, T., Zaccai, N.R., Kikuchi, A., Yabe, T., Tokunaga, K., et al. (1999). Killer cell immunoglobulin receptors and T cell receptors bind peptide-major histocompatibility complex class I with distinct thermodynamic and kinetic properties. J. Biol. Chem. *274*, 28329–28334.

Merritt, E.A., and Bacon, D.J. (1997). Raster3D: photorealistic molecular graphics. Methods Enzymol. *277*, 505–524.

Moretta, A., Bottino, C., Vitale, M., Pende, D., Cantoni, C., Mingari, M.C., Biassoni, R., and Moretta, L. (2001). Activating receptors and coreceptors involved in human natural killer cell-mediated cytolysis. Annu. Rev. Immunol. *19*, 197–223.

Navaza, J. (1994). AmoRe: an automated package for molecular replacement. Acta Crystallogr. A *50*, 157–163.

Nicholls, A., Sharp, K.A., and Honig, B. (1991). Protein folding and association: insights from the interfacial and thermodynamic properties of hydrocarbons. Proteins *11*, 281–296.

O'Callaghan, C.A., Tormo, J., Willcox, B.E., Braud, V.M., Jakobsen, B.K., Stuart, D.I., McMichael, A.J., Bell, J.I., and Jones, E.Y. (1998). Structural features impose tight peptide binding specificity in the nonclassical MHC molecule HLA-E. Mol. Cell *1*, 531–541.

Otwinowski, Z., and Minor, W. (1997). Processing of X-ray diffraction data collected in oscillation mode. Methods Enzymol. *276*, 307–326.

Peruzzi, M., Parker, K.C., Long, E.O., and Malnati, M.S. (1996). Peptide sequence requirements for the recognition of HLA-B*2705 by specific natural killer cells. J. Immunol. *157*, 3350–3356.

Radaev, S., Motyka, S., Fridman, W.H., Sautes-Fridman, C., and Sun, P.D. (2001). The structure of a human type III Fc gamma receptor in complex with Fc. J. Biol. Chem. *276*, 16469–16477.

Reinherz, E.L., Tan, K., Tang, L., Kern, P., Liu, J., Xiong, Y., Hussey, R.E., Smolyar, A., Hare, B., Zhang, R., et al. (1999). The crystal structure of a T cell receptor in complex with peptide and MHC class II. Science *286*, 1913–1921.

Snyder, G.A., Brooks, A.G., and Sun, P.D. (1999). Crystal structure of the HLA-Cw3 allotype-specific killer cell inhibitory receptor KIR2DL2. Proc. Natl. Acad. Sci. USA *96*, 3864–3869.

Tormo, J., Natarajan, K., Margulies, D.H., and Mariuzza, R.A. (1999). Crystal structure of a lectin-like natural killer cell receptor bound to its MHC class I ligand. Nature *402*, 623–631.

Van Duyne, G.D., Standaert, R.F., Karplus, P.A., Schreiber, S.L., and Clardy, J. (1993). Atomic structures of the human immunophilin FKBP-12 complexes with FK506 and rapamycin. J. Mol. Biol. *229*, 105–124.

Vance, R.E., Kraft, J.R., Altman, J.D., Jensen, P.E., and Raulet, D.H. (1998). Mouse CD94/NKG2A is a natural killer cell receptor for the nonclassical major histocompatibility complex (MHC) class I molecule Qa-1(b). J. Exp. Med. *188*, 1841–1848.

Wang, J.H., Smolyar, A., Tan, K., Liu, J.H., Kim, M., Sun, Z.Y., Wagner, G., and Reinherz, E.L. (1999). Structure of a heterophilic adhesion complex between the human CD2 and CD58 (LFA-3) counterreceptors. Cell *97*, 791–803.

Wolan, D.W., Teyton, L., Rudolph, M.G., Villmow, B., Bauer, S., Busch, D.H., and Wilson, I.A. (2001). Crystal structure of the murine NK cell-activating receptor NKG2D at 1.95 A. Nat. Immunol. *2*, 248–254.

Wu, J., Song, Y., Bakker, A.B., Bauer, S., Spies, T., Lanier, L.L., and Phillips, J.H. (1999). An activating immunoreceptor complex formed by NKG2D and DAP10. Science *285*, 730–732.

Yokoyama, W.M. (1998). Natural killer cell receptors. Curr. Opin. Immunol. *10*, 298–305.

Ysern, X., Li, H., and Mariuzza, R.A. (1998). Imperfect interfaces. Nat. Struct. Biol. *5*, 412–414.

Zappacosta, F., Borrego, F., Brooks, A.G., Parker, K.C., and Coligan, J.E. (1997). Peptides isolated from HLA-Cw*0304 confer different degrees of protection from natural killer cell-mediated lysis. Proc. Natl. Acad. Sci. USA *94*, 6313–6318.

Accession

The structure of NKG2D/ULBP3 complex has been deposited in the Protein Data Bank under ID code 1KCG.